Atomic geometry, electronic structure, and vibrational properties of the AlSb(110) and GaSb(110) surfaces

H. M. Tütüncü
Sakarya Üniversitesi, Fen-Edebiyat Fakültesi, Fizik Bölümü, Adapazarı, Turkey

G. P. Srivastava
Department of Physics, University of Exeter, Stocker Road, Exeter EX4 4QL, United Kingdom
(Received 17 August 1998)

We have investigated the atomic geometry and electronic structure of the clean (110) surfaces of AlSb and GaSb using the *ab initio* pseudopotential theory. The calculated atomic geometry for these surfaces is in good agreement with experimental and previous theoretical results. The calculated electronic spectrum for the GaSb(110) surface agrees very well with photoemission results. We have used our atomic geometry to study surface phonons on these surfaces by applying the adiabatic bond-charge model. The calculated phonon spectra for both surfaces compare very well with results obtained from a recent high-resolution electron-energy-loss spectroscopy experiment. The results are used to draw some general trends for surface phonons on III-V(110). [S0163-1829(99)02108-6]

I. INTRODUCTION

Although in general III-V(110) surfaces are among the most widely studied, the majority of experimental and theoretical works have been concentrated on the GaAs(110) and InP(110) surfaces.[1–6] The AlSb(110) and GaSb(110) surfaces have been the least studied crystalline surfaces of binary semiconductors. Atomic geometry and electronic structure of the AlSb(110) surface have not been measured experimentally yet, while only recently the atomic geometry of this surface was studied using the *ab initio* pseudopotential theory.[7] In the case of the GaSb(110) surface, low-energy electron diffraction (LEED) analysis[8] and mass-resolved Rutherford backscattering of He^+ ion experiments[9] were used to determine the relaxed atomic geometry. Surface valence states on GaSb(110) were measured using angle-resolved photoemission experiments.[10–12]

In recent years vibrational properties of III-V(110) surfaces have been investigated using inelastic He atom scattering[13–15] and high-resolution electron energy loss spectroscopy (HREELS) experiments.[16–21] Inelastic He atom scattering can only be used to measure low-energy HREELS (Refs. 20 and 21) has been used to study both low energy and high-energy surface phonon modes. Very recently surface phonons on the (110) surface of AlSb and GaSb have been detected by this technique.[22] On the theoretical side, vibrational properties of III-V(110) surfaces have been studied using an *ab initio* pseudopotential density-functional theory[23,24,7] and an adiabatic bond-charge model.[25–27] In particular, a rotational mode of the GaSb(110) surface was identified using a tight-binding total energy scheme[28] while the phonon dispersion curve of this surface has been calculated using a generalized mass approximation[29] within the *ab initio* pseudopotential density-functional theory.[7]

In the present paper, first of all we present results of an *ab initio* pseudopotential calculation for the relaxed atomic geometry and the electronic structure of AlSb(110) and GaSb(110). The calculated electronic structure for GaSb(110) agrees very well with the angle-resolved photoemission experiment.[10–12] The relaxed geometries are used as input for surface phonon calculations using the adiabatic bond-charge model (BCM). The calculated phonon dispersion curves of both surfaces show very good agreement with results obtained from the recent HREELS experiment.[22] A comparison between the surface phonon displacement patterns on the AlSb(110) and GaSb(110) surfaces reveals a marked qualitative similarity, with quantitative differences in their energy localization explainable in terms of the reduced mass difference between AlSb and GaSb. Additionally, we have observed that some phonon modes on these surface have nearly similar energies and displacement pattern to each other. This similarity is due to the same anion mass. Furthermore, we have attempted to compare our results with those of other III-V(110) surfaces.[27,30,31] From this comparison we find that unlike the (110) surface of InAs, GaP, and InP, the AlSb(110) and GaSb(110) surfaces do not show any gap phonon states deep inside the acoustic-optical gap region. We have also observed that the highest surface optical phonon mode on the AlSb(110) and GaSb(110) surfaces is mainly localized on the cation atoms rather than the anion atoms.

II. ATOMIC GEOMETRY AND ELECTRONIC STRUCTURE

A. Theory: *Ab initio* pseudopotential density-functional theory

The atomic geometry required as input for the phonon studies was calculated within the local-density approximation to the density-functional theory. The electron-ion interaction was dealt with by means of the *ab initio* pseudopotential scheme,[32] employing a basis set of plane waves up to a kinetic energy cutoff of 12 Ry. The surface was modeled within a repeated slab scheme, with a supercell containing seven layers of AlSb (or GaSb) and the equivalent of seven atomic layers of vacuum. The atomic degrees of freedom

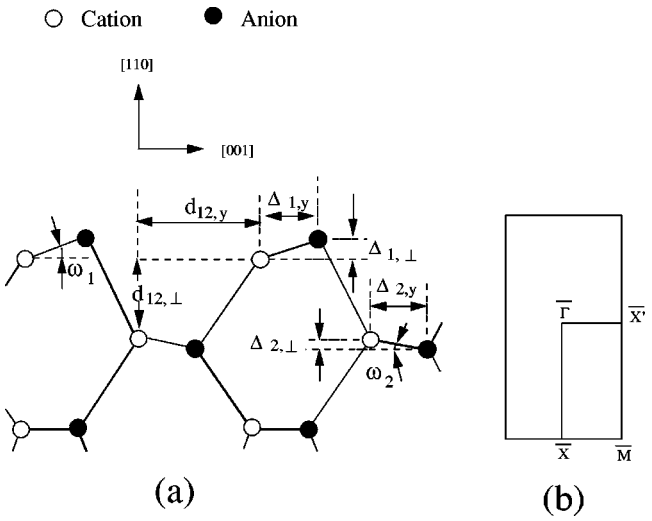

FIG. 1. (a) Schematic relaxed side view of III-V(110). (b) The surface Brillouin zone.

were relaxed by using a conjugate gradient technique, with total energy and forces supplied at each iteration from the solution of the Kohn-Sham equation.

B. Results: Structural and electronic properties

The relaxation of III-V(110) surfaces is well known: the cation-anion chains become tilted with the anions being raised, as shown in Fig. 1. The dangling bonds of the surface cations are empty while the dangling bonds of the surface anions are fully occupied. The first layer cations prefer to be bonded to their group-V nearest neighbors in a nearly planar sp^2 configuration while the first-layer anions prefer a *p*-bonding configuration with their group-III nearest neighbors. The calculated structural parameters of the clean relaxed AlSb(110) and GaSb(110) surfaces are given in Table I. In general, these parameters are in good agreement with the experimental LEED (Ref. 8) studies and a recent *ab initio* calculation.[7] Our calculated bulk lattice constants are 6.08 Å for AlSb and 6.00 Å for GaSb. The buckling angle ω of the top layer for GaSb(110) is found to be 30.12°, in good agreement with experimental studies.[8,9]

Figure 2 shows the electronic structure of the AlSb(110) and GaSb(110) surfaces. The general pattern of the electronic structure of these surfaces is similar to that on other III-V(110) surfaces.[6] For the GaSb(110) surface the calculated electronic structure is in agreement with photoemission measurements.[10–12] We have identified a total of six occupied states on this surface. Only four of them are truly localized surface states: S_1, S_2, S_3, and S_6. The states labeled as S_4 and S_5 are resonant with bulk states. These two states agree well with a recent photoemission experiment.[12] However, we could not identify the S_4 state along the $\overline{X'}$-$\overline{\Gamma}$ and $\overline{\Gamma}$-$\overline{M}$ directions. Our calculated highest occupied electronic state [S_4 for AlSb(110) and S_6 for GaSb(110)], which lies at the lower edge of the fundamental gap region, is made of the dangling bond sp^3-like orbital of the surface Sb atoms and also has a small sp^3-hybrid component at the Sb atoms in the third layer, as shown in Fig. 3. This figure also explains the location of the dangling bond-charges needed for the adiabatic bond-charge model calculation (described in Sec. III). The lowest unoccupied state for both surfaces results from the empty cation dangling bond.

III. LATTICE DYNAMICS

A. Theory: The adiabatic bond-charge model

The phenomenological adiabatic bond-charge model (BCM) was originally developed by Weber to study the lattice dynamics of tetrahedrally coordinated semiconductors.[33,34] This model produces bulk phonon dispersion curves which are in good agreement with experimental neutron scattering data, both for homopolar and heteropolar semiconductors. By using the BCM we study the surface dynamics of AlSb(110) and GaSb(110), within a repeated slab scheme. The supercell used for these calculations contains 22 ions and 44 bond-charges (BCs) located in a slab of 11 atomic layers, and a vacuum region equivalent of nine layers of III-V. Atoms in the top three layers on each side are placed at their relaxed positions, while deeper lying atoms are placed at their bulk positions. The bulk BCs are located between two adjacent atoms, dividing the bond in the ratio 3:5, while the positions of the dangling BCs are obtained from the maximum valence electron density. The chosen

TABLE I. Calculated structural parameters for the AlSb(110) and GaSb(110) surfaces, compared with other theoretical and experimental results. Units: Å for lengths and degrees for angles.

	a_0	$d_{12,\perp}$	$d_{12,y}$	$\Delta_{1,\perp}$	$\Delta_{1,y}$	$\Delta_{2,\perp}$	$\Delta_{2,y}$	ω_1	ω_2
				AlSb(110)					
Present	6.084	1.410	3.459	0.826	1.238	0.184	1.509	33.70	−6.95
ab initio [a]	6.104			0.827	1.249			33.50	
				GaSb(110)					
Present	6.000	1.536	3.455	0.720	1.241	0.078	0.254	30.12	−2.93
ab initio [a]	6.054			0.762	1.268			31.0	
LEED [b]	6.118	1.615	3.629	0.770	1.334			30.0	
He^+ ions [c]								29.0	

[a]Reference 7.
[b]Reference 8.
[c]Reference 9.

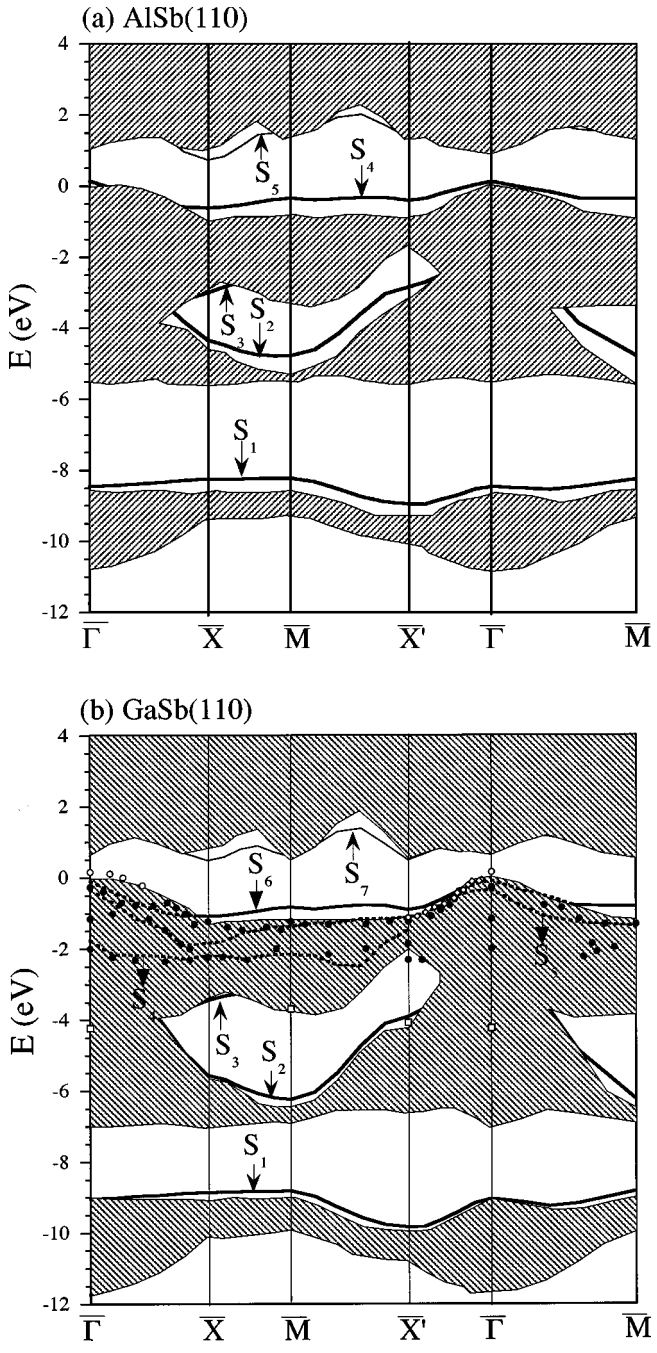

FIG. 2. (a) The electronic band structure of the AlSb(110) clean surface. (b) The electronic band structure of the GaSb(110) clean surface. The projected bulk spectrum is shown by hatched regions. Localized occupied electronic states are shown by thick curves and the localized unoccupied electronic state is shown by the thin curve. Resonant surface states are shown by dashed curves. Photoemission results: open diamonds (Ref. 10), open circles (Ref. 11), closed circles (Ref. 12). Open squares represent previously published data as indicated in Ref. 12.

dangling BCs positions are indicated in Fig. 3 for the (110) surface of AlSb and GaSb, respectively. The interactions included[34,35] in the BCM are the Coulomb interaction between all particles (ion-ion, ion-BC, and BC-BC), a central short-range interaction between the nearest-neighbor particles, and a bond-bending interaction involving the BC-ion-BC angle.

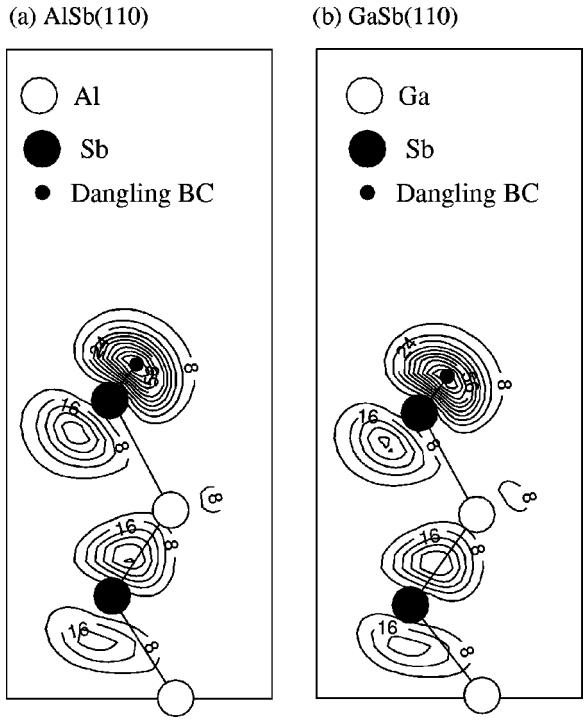

FIG. 3. The electronic charge density for the occupied dangling bond states: (a) for AlSb(110) and (b) for GaSb(110). The figure also explains the location of the dangling bond charges (BCs) needed for the BCM calculation.

B. Results: Surface phonons

1. Phonon spectrum and density of states

The phonon dispersion of AlSb(110) is displayed in Fig. 4(a). The calculated results are shown by thick lines while experimental results, obtained from the HREELS measurement,[22] are shown by open and filled circles. The calculated results along $\overline{\Gamma}$-$\overline{X}$ are in good agreement with experimental results. For this surface, the large gap between the bulk acoustical and optical phonon branches results from the large mass difference between Al and Sb. Three surface-localized phonon states appear throughout the surface Brillouin zone (SBZ) in the acoustic-optical gap range. Two of these lie 0.5 and 1.5 meV below the optic bulk phonon edge in good agreement with the HREELS experiment.[22] The third one lies just above the edge of the bulk acoustic bands. A fourth state appears for a part of the $\overline{\Gamma}$-$\overline{M}$ direction.

The phonon dispersion curve for the GaSb(110) surface is shown in Fig. 4(b). The calculated results along $\overline{\Gamma}$-$\overline{X}$ agree very well with experimental results. Unlike the AlSb(110) surface, there are no surface states on GaSb(110) which lie in the acoustic-optical gap throughout the SBZ. A similar observation was also made by the HREELS experiment[22] along $\overline{\Gamma}$-$\overline{X}$. For the GaSb(110) surface we find a localized state just above the bulk acoustics bands for a part of $\overline{X}$-$\overline{M}$-$\overline{X'}$ and $\overline{\Gamma}$-$\overline{M}$.

In Fig. 5(a) the phonon density of states of AlSb(110) is shown together with the phonon density states of bulk AlSb. The peaks labeled S^1_{AlSb} to S^4_{AlSb} are dominated by atomic vibrations on the surface. The surface phonons in the stomach gap region characterize the peak S^1_{AlSb} while the peaks

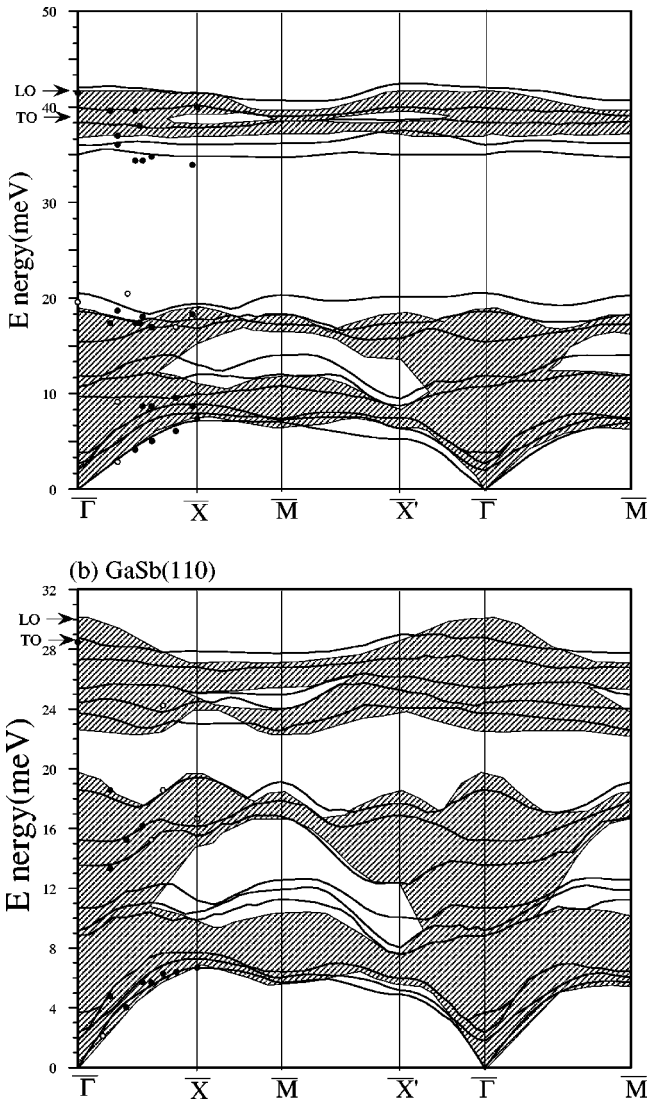

FIG. 4. (a) Dispersion of surface phonon modes on the AlSb(110) surface. (b) Dispersion of surface phonon modes on the GaSb(110) surface. The calculated results are shown by thick solid curves while experimental data from HREELS (Ref. 22) are shown as open and closed circles. Bulk projection is shown by the hatched region.

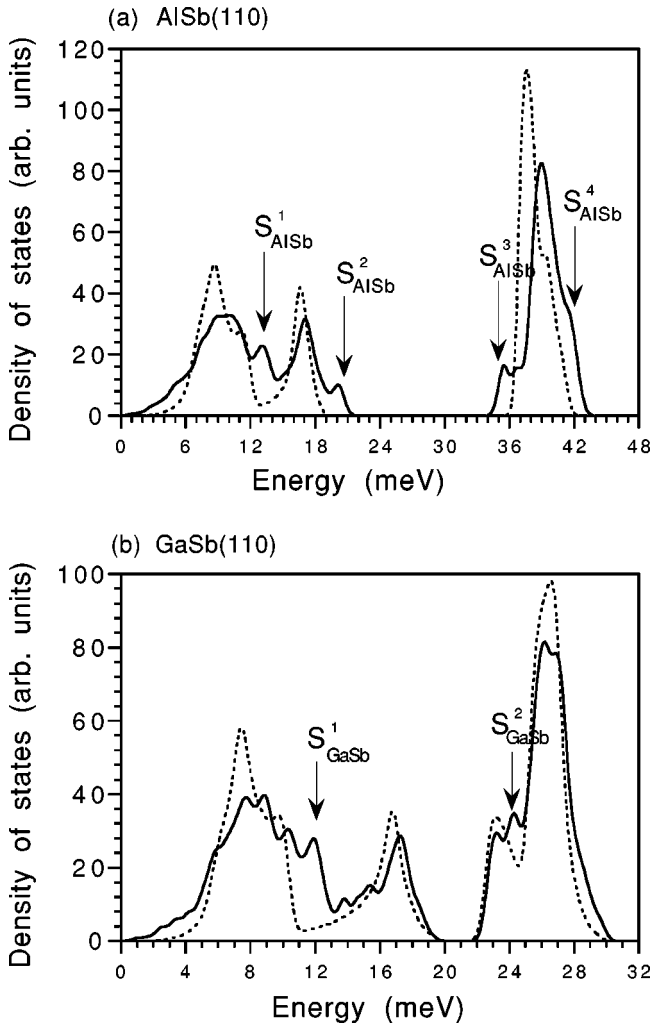

FIG. 5. (a) The density of phonon states on (a) the AlSb(110) surface and (b) the GaSb(110) surface. The solid curve is obtained from the (110) slab supercell calculation with the relaxed surface geometry, while the dotted curve shows the bulk density of states.

S^2_{AlSb} and S^3_{AlSb} are due to the phonon modes in the acoustic-optical gap region. The shoulder S^4_{AlSb} results from the highest surface optical phonon modes.

The phonon density of the states of GaSb(110) surface is displayed in Fig. 5(b). For comparison, the phonon density of states for bulk GaSb is shown by the dashed curve. The peaks labeled S^1_{GaSb} and S^2_{GaSb} are characterized by the atomic vibrations on the surface. The peak S^1_{GaSb} is mainly due to stomach gap phonon modes. The peak S^2_{GaSb} is dominated by the optical surface phonons along the $\bar{\Gamma}$-$\bar{X}$ and $\bar{\Gamma}$-$\bar{M}$ directions [see Fig. 4(b)].

2. Polarization and localization of surface modes

We will first discuss the phonon mode at $\bar{\Gamma}$. The calculated zone-center surface phonons on the AlSb(110) and GaSb(110) surfaces are summarized in Table II. The calculated results are also compared with a recent *ab initio* calculation[7] and the HREELS experiment.[22] In this table, atomic vibrations along $[\bar{1}10]$, i.e., along the III-V zigzag chain direction, are represented as A'' modes, and vibrations perpendicular to the chain direction are represented as A'.

The rotational phonon mode of the AlSb(110) and GaSb(110) surfaces is identified at energies 9.70 and 8.86 meV, respectively. The atomic displacement pattern of this phonon mode is shown in Fig. 6(a). This phonon mode for both surfaces is mainly dominated by opposing motion of atoms in the top two layers along the surface normal direction. The rotational phonon mode of GaSb(110) compares very well with the phonon mode at 9.0 meV in the work of Wang and Duke.[28] For both surfaces we have identified an anionic phonon mode: at 15.47 meV for AlSb(110) and 15.24 meV for GaSb(110). This phonon mode mainly comes from opposing motion of Sb atoms in the top two layers with components both in the [110] and [001] directions as can be seen in Fig. 6(b). The similarity in the energy localization of this phonon mode for both surfaces is due to the same anion mass in both materials.

TABLE II. Calculated surface phonon frequencies (in meV) on AlSb(110) and GaSb(110) at the $\bar{\Gamma}$ point and their comparison with a recent HREELS experiment (Ref. 22) and *ab initio* calculation (Ref. 7). Atomic vibrations along $[\bar{1}10]$, i.e., along the III-V zigzag chain direction, are represented as A'' modes, and vibrations in the plane perpendicular to the chain direction as A'.

AlSb(110)								
Source	A'' modes			A' modes				
Present	10.71	35.02	39.90	9.70	15.44	20.54	36.03	42.00
ab initio [a]		36.0					35.7	
HREELS [b]						19.60		41.5
GaSb(110)								
Source	A'' modes			A' modes				
Present	9.17	24.44	27.30	8.85	15.24	18.60	25.40	28.80
Tight-binding[c]				9.0				
ab initio [a]								$\sim$ 29.5
HREELS [b]								28.5

[a]Reference 7.
[b]Reference 22.
[c]Reference 8.

Three modes are found at 20.54, 35.02, and 36.03 meV in the acoustic-optical gap region of AlSb. The atomic displacement patterns of these phonon modes are shown in Fig. 7. The intermediate gap phonon mode is of A'' mode and corresponds to the top-layer atoms vibrating against each other in the zigzag chain direction. This phonon mode was identified at 25.85 meV for InAs(110), 31.03 meV for InP(110), and 38.79 meV for GaP(110). For these surfaces the mass of the anion is smaller than the mass of the cation, leading to a larger displacement from the first layer anion. But the reverse is true for the AlSb(110) surface due to smaller cation mass. The gap phonon mode at 20.54 meV is localized on the first-layer cations. The gap phonon mode at 36.03 meV is characterized by opposing motion of the top-layer and second-layer atoms in the surface normal direction while the atoms on the top two layers vibrate against each other in the [001] direction. As can be seen from Fig. 7, this phonon mode is mainly localized on the cation atoms due to the large mass difference between Al and Sb atoms. For this mode there is also a large amplitude of atomic vibrations in the third-layer Al atoms.

For the GaSb(110) surface there are no gap phonon modes at the $\bar{\Gamma}$ point in the acoustic-optical gap region. However we observe that the phonon modes at 24.44 and 25.40 meV on the GaSb(110) surface have displacement patterns similar to the phonon modes at 35.02 and 36.03 meV on the AlSb(110) surface. The average ratio of these frequencies is approximately 1.42, which is equal to the ratio of the square root of the reduced masses between AlSb and GaSb. This clearly shows that the energy locations of these states can be linked to the square root of the reduced masses.

We have identified the Fuchs-Kliewer phonon mode at 28.80 meV for GaSb(110) and at 42.00 meV for AlSb(110). The atomic displacement pattern of this phonon mode also is plotted in Fig. 8. For both surfaces this phonon mode corresponds to first-layer atoms vibrating against second-layer at-

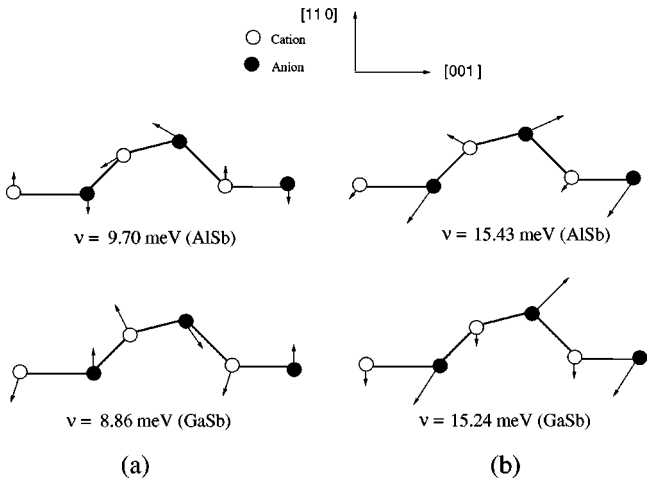

FIG. 6. (a) Atomic displacement patterns of the rotational phonon mode and (b) anionic phonon mode on the AlSb(110) and GaSb(110) surfaces at the $\bar{\Gamma}$ point.

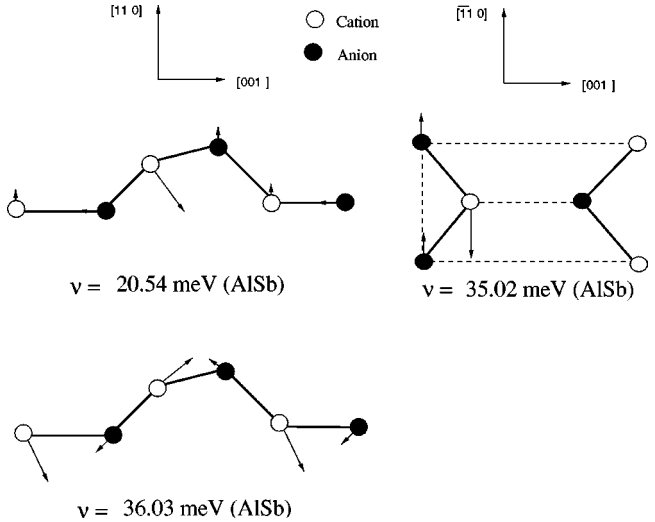

FIG. 7. Atomic displacement patterns of gap phonon modes on the AlSb(110) surface at the $\bar{\Gamma}$ point.

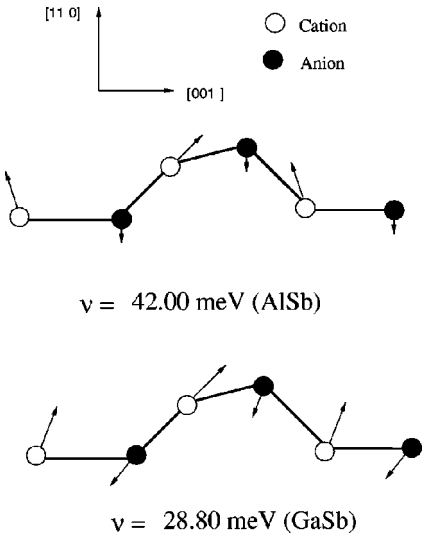

FIG. 8. Atomic displacement patterns of the Fuchs-Kliewer phonon mode of AlSb(110) and GaSb(110) surfaces at the $\overline{\Gamma}$ point.

oms in the surface normal direction. Once again, the energy difference in the energy location of this phonon mode for these surfaces can be linked to the square root of the reduced masses.

The calculated dispersion of modes on both surfaces along $\overline{\Gamma}$-$\overline{X}$ agrees well with the recent HREELS measurements.[22] The Rayleigh (RW) mode at $\overline{X}$ is found at 7.17 meV for AlSb(110) and 6.70 meV for GaSb(110), which can be compared with the phonon modes at 7.5 meV and 6.7 meV in the HREELS experiment of Nienhaus.[22] This phonon mode for these surfaces is due to the motion of top-layer cations and second-layer anions with components both in the [110] and [001] directions, while the first-layer anions vibrate in the zigzag chain direction. The energy difference in the RW phonon mode of these surfaces can be related to the square root of the total masses. The ratio of the RW mode of these surfaces is 1.10, which is very close to the ratio of the square root of the total masses 1.13. A similar observation was made for other III-V(110) surface in one of our previous papers.[30] The stomach gap phonon modes at 13.00 meV for AlSb(110) and 11.18 meV for GaSb(110) correspond to the first-layer cations vibrating against the second-layer anions in the [001] direction, while the first-layer anions and second-layer cations move against each other in the zigzag chain direction. The frequencies at 16.98 meV for AlSb(110) and 16.16 meV for GaSb(110) are anionic modes at the $\overline{X}$ point and correspond to the first-layer anions vibrating in the zigzag chain direction while the second layer anions are displaced in the [001] direction.

The highest surface optical phonon mode of the AlSb(110) surface at the $\overline{X}$ point is found at 41.45 meV. This phonon mode is mainly localized on the first-, second-, and third-layer Al atoms. The mode is dominated by the opposing motion of the first- and third-layer Al atoms in the surface normal direction, while the second-layer Al atoms vibrate against the first-layer Sb atoms in the zigzag chain direction. For the GaSb(110) surface this phonon mode is due to the motion of the first-layer Ga and second-layer Sb atoms in the [001] direction, while second-layer Ga and first-layer Sb atoms move in the zigzag chain direction.

The calculated surface phonons at $\overline{X'}$ on the AlSb(110) and GaSb(110) surfaces are listed in Table III. There are three surface acoustic phonon modes near the bottom of the bulk acoustic bands, as observed for other III-V(110) surfaces.[27,30] These frequencies are predicted at energies 5.27, 6.34, and 7.43 meV for AlSb(110) and 4.90, 5.20, and 6.00 meV for GaSb(110). These three phonon modes for the two surfaces share similar displacement patterns. The RW phonon modes at 5.27 meV for AlSb(110) and 4.90 meV for GaSb(110) are due to the parallel motion of top-layer atoms in the [001] direction while the second-layer atoms vibrate parallel to each other in the surface normal direction. The second surface acoustic phonon mode on both surfaces is characterized by a pure shear-horizontal displacement pattern. The phonon modes at 7.43 meV for AlSb(110) and 6.00 meV for GaSb(110) have a displacement pattern opposite to the RW modes. Because of the large difference between anion mass and cation mass ($m_a > m_c$), these three modes have large displacements from Sb atoms for both surfaces.

At the $\overline{X'}$ point we have found an anionic phonon mode at 9.48 meV in the stomach gap region on AlSb(110) (see Fig. 9). For the GaSb(110) surface this phonon mode shows a mixed polarization behavior. The mode also includes a large displacement pattern from the first- and second-layer cations as shown in Fig. 9. The phonon mode at 20.17 meV has a similar displacement pattern to the phonon mode at 20.54

TABLE III. Calculated surface phonon frequencies (in meV) on AlSb(110) and GaSb(110) at the $\overline{X'}$ point and their comparison with a recent *ab initio* calculation. Atomic vibrations along $[\overline{1}10]$, i.e., along the III-V zigzag chain direction, are represented as A'' modes, and vibrations in the plane perpendicular to the chain direction as A'.

					AlSb(110)				
Source	A'' modes		A' modes						
Present	6.34	35.02	5.27	7.43	9.48	20.17	35.00	37.53	42.40
					GaSb(110)				
Source	A'' modes		A' modes						
Present	5.20	24.44	4.90	6.00	10.07	17.68	25.40	26.16	29.00
ab initio [a]			$\sim$ 4.6		$\sim$ 10.5				$\sim$ 31.0

[a]Reference 7.

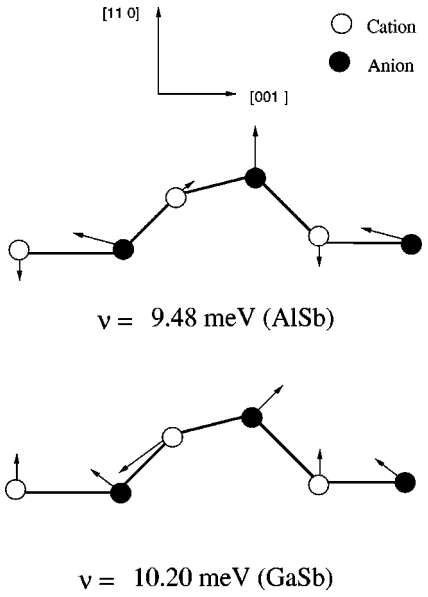

FIG. 9. Atomic displacement patterns of the stomach gap phonon mode on AlSb(110) and GaSb(110) surfaces at the $\overline{X'}$ point.

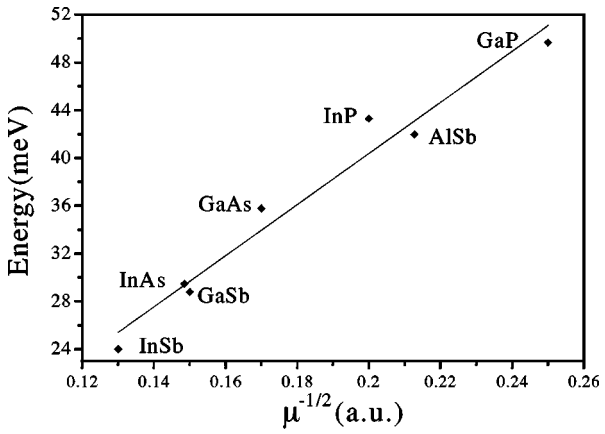

FIG. 10. The Fuchs-Kliewer frequency of III-V(110) surfaces at the $\overline{\Gamma}$ point against the square root of the reduced mass (μ) of the cation and anion.

meV at the $\overline{\Gamma}$ point, while the second gap phonon mode has a displacement pattern similar to that for the phonon mode at 35.03 meV at the $\overline{\Gamma}$ point. The highest surface optical phonon mode is found at 42.40 meV for AlSb(110) and 29.00 meV for GaSb(110). This phonon mode comes from the motion of the top-layer cations with components both in the [110] and [001] directions while the second-layer anions move in the [001] direction. For this mode there is also a large amplitude of atomic vibrations in the third-layer cations.

3. Similarities and mass trends

The first point to note is that the rotational mode predicted by Wang and Duke[28] can be identified for AlSb(110) and GaSb(110) surfaces. We also identified this phonon mode for the (110) surfaces of GaAs, InP, InAs, GaP, and InSb in our previous publications.[30,31] This mode for all III-V(110) surfaces can be classified as a surface optical mode but lies in the bulk acoustic range.

All of the III-V(110) surfaces we have studied show three acoustical phonon modes in the $\overline{\Gamma}$-$\overline{X'}$ direction. The intermediate acoustic surface phonon mode always has A'' polarization while the others have the A' character. For the (110) surface of InAs, InP, and GaP we found a gap phonon state in the middle of the acoustic-optical gap region while for the AlSb(110) surface the gap phonon states appear very close to bulk optical phonons and acoustic phonons. Moreover, we have not observed any gap phonon states for the GaSb(110) surface. Our results therefore indicate that the gap phonon states can be obtained well inside the acoustic-optical gap region if the mass of the cation is bigger than the mass of the anion.

Figure 10 illustrates the Fuchs-Kliewer frequency of III-V(110) surfaces against the square root of the inverse reduced mass of the surface cation and anion. For all the considered III-V(110) surfaces we observed a nearly linear behavior in this figure. This linear behavior shows that the effective force constant for this mode on all the considered surfaces is very similar and the difference in the energy of this mode is mainly due to the reduced mass difference. The highest surface optical phonon mode on all the III-V(110) surfaces lies above the projected bulk bands at the $\overline{X'}$. It is observed that this phonon mode is mainly characterized by larger displacements of second-layer anions for the (110) surface of InAs, GaP, and InP with $m_{\text{anion}} < m_{\text{cation}}$. However, this mode is mainly dominated by larger displacements of the first- and third-layer cations for the AlSb(110) and GaSb(110) surfaces for which $m_{\text{anion}} > m_{\text{cation}}$.

IV. SUMMARY

In this paper, the atomic geometry and electronic structure of (110) surface of AlSb and GaSb were investigated and discussed by employing an *ab initio* pseudopotential theory. We then investigated the vibrational properties of these surfaces by applying the adiabatic bond-charge model to our relaxed atomic geometry and the dangling bond-charge positions. In general, the geometrical results are in agreement with earlier theoretical calculations. In the case of GaSb, the calculated electronic structure agrees very well with experimental results.

The calculated surface phonon dispersion curves for both surfaces agree well with recent HREELS results. Furthermore, the calculated frequencies at the symmetry points on the surface Brillouin zone are also in good overall agreement with recent *ab initio* phonon calculations. From a comparison of the surface phonon modes on these surfaces, we found that the displacement patterns of a large variety of surface phonon modes are similar for both surfaces and that the difference in their energies can be explained either in terms of the reduced mass or the total mass differences. Moreover, some phonon modes of these surfaces with similar energies have similar displacement patterns, which is explained to be due to the same anion atoms.

Because of the structural similarity of the III-V(110) surfaces, certain trends are obtained for surface phonons. The obtained trends can be summarized as follows: first, all the considered (110) surfaces exhibit three acoustical phonon

modes with similar polarization characters at the $\overline{X'}$ point. Second, the rotational phonon mode at the $\overline{\Gamma}$ point is identified for all the III-V(110) surfaces. Third, comparing the Fuchs-Kliewer frequency of the III-V(110) surfaces, it is found that the effective force constant for this mode on all the considered surfaces is very similar and the difference in the energy of this mode is mainly due to the reduced mass difference.

Because of smaller cation mass the AlSb(110) and GaSb(110) surfaces are found to show somewhat different dynamical behavior than the (110) surface of InAs, GaP, and InP. These differences can be summarized as follows. First, for AlSb(110) and GaSb(110) no surface phonon states are found to lie well inside the bulk acoustic-optical gap region. Second, the gap phonon modes on the AlSb(110) surface are mainly localized on the cation atoms while the corresponding phonon modes on the (110) surface of InAs, GaP, and InP are mainly localized on the anion atoms. Finally, we generally observe that the highest surface optical phonon frequency at $\overline{X'}$ involves larger displacements from the second-layer anions when $m_{\text{anion}} < m_{\text{cation}}$ and from the first-layer cations when $m_{cation} < m_{anion}$.

[1] A. Huijer, J. van Laar, and T. L. van Rooy, Phys. Lett. **65A**, 337 (1978).
[2] C. B. Duke, R. J. Meyer, A. Paton, P. Mark, Phys. Rev. B **18**, 4225 (1978).
[3] A. Kahn, Surf. Sci. Rep. **3**, 193 (1983).
[4] L. Smit, T. E. Derry, and J. F. van der Veen, Surf. Sci. **150**, 245 (1985).
[5] W. K. Ford, T. Guo, D. L. Lessor, and C. B. Duke, Phys. Rev. B **42**, 8952 (1990).
[6] A. Umerski and G. P. Srivastava, Phys. Rev. B **51**, 2334 (1995).
[7] C. Eckl, J. Fritsch, P. Pavone, and U. Schröder, Surf. Sci. **394**, 47 (1997); and private communications.
[8] C. B. Duke, A. Paton, and A. Kahn, Phys. Rev. B **27**, 3436 (1983).
[9] L. Smit, R. M. Tromp, J. F. van der Veen, Phys. Rev. B **29**, 4814 (1985).
[10] R. Manzke, H. P. Barnscheidt, C. Janowitz, and M. Skibowski, Phys. Rev. Lett. **58**, 610 (1987).
[11] X. D. Zhang, R. Leckey, J. Riley, J. Faul, L. Ley, Phys. Rev. B **48**, 5300 (1993).
[12] W. Oueini, M. Banouni, and G. Leveque, Surf. Sci. **410**, 132 (1198).
[13] U. Harten and J. P. Toennies, Europhys. Lett. **4**, 833 (1987).
[14] R. B. Doak and D. B. Nguyen, J. Electron Spectrosc. Relat. Phenom. **44**, 205 (1987).
[15] M. B. Nardelli, D. Cvetko, V. De Renzi, L. Floreano, A. Morgante, M. Peloi, and F. Tommasini, Phys. Rev. B **52**, 16 720 (1995).
[16] L. H. Dubois and G. P. Schwartz, Phys. Rev. B **26**, 794 (1982).
[17] A. Ritz and H. Lüth, Phys. Rev. Lett. **52**, 1242 (1984).
[18] M. G. Betti, U. del Pennino, and C. Mariani, Phys. Rev. B **39**, 5887 (1989).
[19] Y. Chen, J. C. Hermanson, and G. J. Lapeyre, Phys. Rev. B **39**, 12 682 (1989).
[20] H. Nienhaus and W. Mönch, Phys. Rev. B **50**, 11 750 (1994).
[21] H. Nienhaus and W. Mönch, Surf. Sci. **328**, L561 (1995).
[22] H. Nienhaus, Phys. Rev. B **56**, 13 194 (1997).
[23] J. Fritsch, P. Pavone, and U. Schröder, Phys. Rev. Lett. **71**, 4194 (1993).
[24] J. Fritsch, P. Pavone, and U. Schröder, Phys. Rev. B **52**, 11 326 (1995).
[25] P. Santini, L. Miglio, G. Benedek, U. Harten, P. Ruggerone, and J. P. Toennies, Phys. Rev. B **42**, 11 942 (1990).
[26] P. Santini, L. Miglio, G. Benedek, and P. Ruggerone, Surf. Sci. **241**, 346 (1991).
[27] H. M. Tütüncü and G. P. Srivastava, Phys. Rev. B **53**, 15 675 (1996).
[28] Y. R. Wang and C. B. Duke, Surf. Sci. **205**, L755 (1988).
[29] P. Giannozzi, S. de Gironcoli, P. Pavone, and S. Baroni, Phys. Rev. B **43**, 7231 (1991).
[30] H. M. Tütüncü; and G. P. Srivastava, J. Phys. Chem. Solids **58**, 685 (1997).
[31] H. M. Tütüncü, M. Çakmak, and G. P. Srivastava Appl. Surf. Sci. **123**, 146 (1998).
[32] G. B. Bachelet, D. R. Hamann, and M. Schlüter, Phys. Rev. B **26**, 4199 (1982).
[33] W. Weber, Phys. Rev. Lett. **33**, 371 (1974).
[34] K. C. Rustagi and W. Weber, Solid State Commun. **18**, 673 (1979).
[35] S. K. Yip and Y. C. Chang, Phys. Rev. B **30**, 7037 (1984).